

# Human Skeletal Muscle Stem Cell Antiinflammatory Activity Ameliorates Clinical Outcome in Amyotrophic Lateral Sclerosis Models

Laura Canzi,<sup>1,2</sup> Valeria Castellaneta,<sup>3</sup> Stefania Navone,<sup>1</sup> Sara Nava,<sup>1</sup> Marta Dossena,<sup>1</sup> Ileana Zucca,<sup>4</sup> Tiziana Mennini,<sup>3</sup> Paolo Bigini,<sup>3\*</sup> and Eugenio A Parati<sup>1\*</sup>

<sup>1</sup>Department of Cerebrovascular Disease, IRCCS Foundation, Neurological Institute “C. Besta,” Milan, Italy; <sup>2</sup>Department of Biotechnology and Biosciences, University of Milano-Bicocca, Milan, Italy; <sup>3</sup>Department of Molecular Biochemistry and Pharmacology, Mario Negri Institute for Pharmacological Research, Milan, Italy; and <sup>4</sup>Science Direction Unit, IRCCS Foundation, Neurological Institute “C. Besta,” Milan, Italy

Mesenchymal stem cell (MSC) therapy is considered one of the most promising approaches for treating different neurodegenerative disorders, including amyotrophic lateral sclerosis (ALS). We previously characterized a subpopulation of human skeletal muscle–derived stem cells (SkMSCs) with MSC-like characteristics that differentiate into the neurogenic lineage *in vitro*. In the present study, we evaluated the SkMSC therapeutic effects in the most characterized model of spontaneous motor neuron degeneration, the Wobbler (Wr) mouse. Before evaluating the therapeutic efficacy in the Wr mouse, we followed the route of SkMSCs at different times after intracerebroventricular injection. Two exogenous tracers, superparamagnetic iron oxide (SPIO) nanoparticles and Hoechst 33258, were used for the *in vivo* and *ex vivo* tracking of SkMSCs. We found that the loading of both Hoechst and SPIO was not toxic and efficiently labeled SkMSCs. The magnetic resonance imaging (MRI) system 7 Tesla allowed us to localize transplanted SkMSCs along the whole ventricular system up to 18 wks after injection. The *ex vivo* Hoechst 33258 visualization confirmed the *in vivo* results obtained by MRI analyses. Behavioral observations revealed a fast and sustained improvement of motor efficacy in SkMSC-treated Wr mice associated with a relevant protection of functional neuromuscular junctions. Moreover, we found that in SkMSC-treated Wr mice, a significant increase of important human antiinflammatory cytokines occurred. This evidence is in accordance with previous findings showing the bystander effect of stem cell transplantation in neurodegenerative disorders and further strengthens the hypothesis of the possible link between inflammation, cytotoxicity and ALS.

Online address: <http://www.molmed.org>

doi: 10.2119/molmed.2011.00123

## INTRODUCTION

Amyotrophic lateral sclerosis (ALS) is an adult-onset neurodegenerative disorder affecting upper and lower motor neurons and leading to muscular atrophy and paralysis. The pathological hallmarks of ALS are the atrophy of dying motor neurons, which are surrounded by reactive astrocytes and microglia (1). Riluzole is the only drug approved by

the U.S. Food and Drug Administration for the treatment of ALS patients. However, its effect is both minimal and controversial (2). In the emerging field of regenerative medicine, mesenchymal stem cell (MSC) transplantation holds the promise of treating a variety of degenerative diseases where no specific or effective treatment is currently available (3). MSCs can differentiate into multiple

mesoderm-type and non-mesoderm-type cells, including neuronal-like cells (4–6).

Indeed, a previous study in our laboratory demonstrated that human adult skeletal muscle–derived stem cells (SkMSCs) may also differentiate into neurogenic cell lineages (7). In this study, we demonstrated that human fetal skeletal muscle may contain MSC-like cells endowed with neurogenic differentiation capabilities *in vitro*.

Moreover, considering the antiinflammatory and immunomodulatory properties and hypoinflammatory nature of MSCs (8), we hypothesized that muscle may be a tissue source for the isolation of MSCs for development of cell-based therapies for human neurodegenerative diseases with multifactorial features such as ALS. The potential of stem cell therapy has already been demonstrated in a

\*PB and EAP contributed equally to this work.

Address correspondence to Laura Canzi, IRCCS, Neurological Institute “C. Besta,” Via Celoria, 1 20133 Milan, Italy; Phone: +39-02-23942272; Fax: +39-02-23942272; E-mail: [laura.canzi@istituto-besta.it](mailto:laura.canzi@istituto-besta.it).

Submitted April 1, 2011; Accepted for publication November 3, 2011; Epub ([www.molmed.org](http://www.molmed.org)) ahead of print November 4, 2011.

familial model of ALS—the transgenic mutant superoxide dismutase 1 (SOD1) mouse (9).

Thus, in the present study, the possible therapeutic effects of human SkmSC transplantation by a single bilateral intracerebroventricular administration was evaluated in a well-characterized murine model of spontaneous motor neuron degeneration, the Wobbler (Wr) mouse (10). The Wr mouse carries a homozygous missense mutation (L967Q) in the vacuolar protein sorting 54 (*Vps54*) gene that codifies for a protein involved in the retrograde transport from late endosomes to the Golgi apparatus (11). Although this mutation is not yet associated with any case of ALS, it leads to early motor neuron disorder that shares the many neuropathological and clinical features found in patients with ALS. Moreover, the evidence that chronic treatment with Riluzole improves motor behavior, prevents biceps muscle atrophy and decreases the amount of motor neuron loss in Wr mice makes it an interesting and reliable model to investigate the pathological mechanisms involved in sporadic ALS and the effect of a wide range of therapeutic approaches (12,13).

Our results show that treatment of Wr mice with human SkmSCs during the presymptomatic phase can delay disease symptoms of Wr mice, possibly via immunomodulation and inhibition of inflammatory response. We hope that a greater understanding of human SkmSC therapeutic action may create new perspectives in the pharmacological treatment of ALS.

## MATERIALS AND METHODS

### SkmSC Isolation, Culture and Differentiation

SkmSCs were derived from muscles of 12- to 16-wk-old fetuses obtained following the ethical guidelines of the European Network for Transplantation (NECTAR) and were processed as previously reported (7). Single cells are plated in the presence of 20 ng/mL EGF and

10 ng/mL basic fibroblast growth factor (bFGF) in a serum-free stem-cell medium optimized for neural stem cell growth supplemented with Noggin (100 ng/mL; R&D Systems, Minneapolis, MN, USA) (growth medium) (14). The experimental protocol was approved by the ethics committee of the Foundation IRCCS Neurological Institute “C. Besta,” Milan, Italy, and the Foundation IRCCS Policlinico-Mangiagalli-Regina Elena, Milan Italy.

### Fluorescence-Activated Cell Sorter (FACS) Analysis

The phenotypic characterization of SkmSCs was evaluated by flow cytometry (fluorescence-activated cell sorter [FACS]) as described previously [7] with CD44, CD166, CD73 (BD Pharmingen, San Jose, CA, USA), CD56, CD133/2, CD34 (Miltenyi Biotec, Bisley, Surrey, UK), CD105 (ABDSerotec, Raleigh, NC, USA) and CD90 (Millipore, Temecula, CA, USA).

### Immunocytochemistry

For differentiation assay, SkmSCs were plated as previously reported (7). Cell composition was analyzed by means of immunostaining with lineage-specific antibodies: glial fibrillary acidic protein (GFAP) (rabbit, 1:500); NG2 (new glue 2; CSPG4, chondroitin sulfate proteoglycan 4) (rabbit, 1:200); class III  $\beta$  tubulin (mouse, 1:100) (Chemicon, Temecula, CA, USA) and Nestin (mouse 1:100; R&D Systems).

### Magnetic Labeling of Human SkmSCs

Superparamagnetic iron oxide (SPIO) labeling (Endorem AMI-25; Guerbet; particle size, 80–150 nm; stock solution, 11.2 mg Fe/mL) was performed as previously reported (15).

### Hoechst 33258 Dye Staining of SPIO-Labeled Human SkmSCs

SPIO-labeled SkmSC cultures in 12-well plates were incubated with 2  $\mu$ mol/L Hoechst 33258 reagent (Molecular Probes, Eugene, OR, USA) for 1 h at 37°C in the dark. After incubation, the cells

were plated on matrigel-coated glass-chamber slides (Nunc, Naperville, IL, USA) in serum-free growth medium for 2 d and fixed in 4% paraformaldehyde (PFA). After that, SPIO efficiency was analyzed by means of immunostaining with anti-dextran antibody (STEMCELL Technologies Inc., Vancouver, BC, Canada).

### Animals

Procedures involving animals and their care were conducted in conformity with the institutional guidelines that are in compliance with national and international laws and policies (16–18) and the National Institutes of Health (NIH) *Guide for the Care and Use of Laboratory Animals* (19). The protocol for the use of laboratory animals was approved by the Italian Ministry of Health and by an internal ethical committee.

Wr mice were originally obtained from NIH genetics and then bred at Charles River Italy, Calco (LC), Italy. Heterozygous founders were designed by genotyping (20).

### Experimental Schedule

The recruitment of Wr mice for our studies was carried out after clear diagnosis of the disease on the basis of phenotype analysis (fourth week of life). Age-matched healthy littermates, homozygous for the wild-type form of the *Vps54* gene, were selected after genotyping (12).

For each experimental group, the same number of males and females were recruited, since no sex-related difference in the evolution of the Wr disease was reported. A schematic timeline of the experimental plan is shown in Supplementary data 1: Experimental Plan Timeline.

### Human SkmSC Transplantation in ALS Animal Models

For injection of SkmSCs, mice were anesthetized using isoflurane and placed in a stereotaxic frame. The head was shaved and a ~1-cm incision was made to expose the skull. By use of a micro-

drill, two 1- to 2-mm holes were produced to allow two intracerebroventricular injections (stereotaxic coordinates of 4-wk-old control mice  $\pm$  1.0 mm lateral to bregma,  $\pm$  0 mm rostro-caudal to bregma and 3.0 mm deep from the skull surface; stereotaxic coordinates of 4-wk-old Wr mice  $\pm$  0.8 mm lateral to bregma, + 0.5 mm rostro-caudal to bregma and 2.5 mm deep from the skull surface). As sham controls, animals were injected with 5  $\mu$ L phosphate-buffered saline (PBS) without cells. All injections were performed with a Hamilton syringe. A total of  $5 \times 10^5$  cells with a total volume of microliters was injected per animal. No immunosuppression was given, since human fetal cells with low immunogenicity were used.

### Magnetic Resonance Imaging Experiments

Magnetic resonance imaging (MRI) scanning was performed by a 7 Tesla and 30-cm bore Bruker spectrometer (BioSpin 70/30 USR) equipped with a surface mouse brain radio-frequency (RF) coil. A three-orthogonal plane gradient echo TriPilot scan (TriPilot protocol of ParaVision 4.0 software; Bruker BioSpin MRI GmbH, Ettlingen, Germany) was used as a geometric reference to locate the olfactory bulbs, and the sections were chosen from this scan. T2-weighted images (axial, sagittal, coronal; rapid acquisition with refocusing echoes (RARE) factor = 8, time of repetition (TR) = 3.3 s, time to echo (TE) = 54 ms, interecho time = 13.5 ms, field-of-view (FOV) =  $2.2 \times 2.2$  cm<sup>2</sup>, data matrix  $256 \times 256$ , slice thickness = 1 mm) were acquired to visualize anatomical details. T2\*-weighted images (axial; FLASH Flip Angle = 30 degrees, TR = 1 s, TE = 7 ms, FOV =  $1.8 \times 1.8$  cm<sup>2</sup>, data matrix  $128 \times 128$ , slice thickness = 0.6 mm) were acquired to visualize the susceptibility artifacts due to the presence of iron. To acquire the image of the spinal cord with a gray-white matter contrast, T1-weighted images (axial; spin echo, TR = 300 ms, TE = 11.7 ms, FOV =  $2.7 \times 2.7$  cm<sup>2</sup>, data matrix  $256 \times 256$ , slice thickness = 0.5 mm) were acquired.

### Disease Progression Assessment

Behavioral trials were performed according to the procedure described previously (21).

### Motor Neuron and Neuromuscular Junction Counting

Choline acetyl transferase (ChAT)-positive neuron counting was carried out in the cervical region corresponding to C2–C5 in 7- and 9-wk-old Wr and age-matched controls ( $n = 5$  for each group), according to the procedure previously described (22).

Neuromuscular junction counting was performed by employing bromo indoxyl acetate dye-staining methods as described (23).

### Immunohistochemistry

The mouse astroglial markers were revealed by antibodies against GFAP (mouse monoclonal antibody; Immunological Sciences, Rome, Italy; dilution 1:1,000), CD11b (rat monoclonal antibody OX 42; Serotec, Oxford, UK; dilution 1:300). Sections were observed with an Olympus Fluoview microscope BX61 with the confocal system FV500. Pseudocolors were used, and the signals from the three different channels were automatically merged by Olympus Fluoview software.

### Real-Time Quantitative Polymerase Chain Reaction

RNA extractions were performed on four total brains and cervical spinal cords of 6-wk-old SkmSC-transplanted Wr mice (2 wks after intracerebroventricular transplant with SkmSCs), on four total brains and cervical spinal cords of 6-wk-old Wr mice and on controls of SkmSCs cultured as described above. Real-time polymerase chain reaction (PCR) was performed using the Human Inflammatory Cytokines & Receptors RT<sup>2</sup> Profiler™ PCR Array (SuperArray Bioscience Corporation, Frederick, MD, USA).

Pathway-focused gene expression analysis was performed with the PCR Array System and the PCR Array Data Analysis Web Portal. RT<sup>2</sup> Profiler™ PCR

Arrays were done on separate cDNAs at least three times.

### Bio-Plex Assay

Protein extractions were performed on four total brains and cervical spinal cords of 6-wk-old SkmSC-transplanted Wr mice (2 wks after intracerebroventricular transplant with SkmSCs), on four total brains and cervical spinal cords of 6-wk-old Wr mice and on controls of SkmSCs cultured as described above, with Bio-Plex cell lyses kit (Bio-Rad, Hercules, CA, USA) following the manufacturer's instructions. Two human cytokines (hIL-13 Bio-Plex human group I region 56, hIL-10 Bio-Plex human group I region 51) were estimated by using Bio-Plex Protein Array System (Bio-Rad). Samples were diluted in lyses buffer plus bovine serum albumin 0.5% at a final concentration of 0.5 and 10 mg/mL. The assay was performed according to the manufacturer's instructions. Data have been normalized with background fluorescence intensity.

### Statistical Analysis

Numerical values are expressed as mean  $\pm$  standard deviation (SD). Comparisons of parameters were performed with a Student *t* test. Comparisons of parameters among three groups were made with a one-way analysis of variance test.  $P < 0.05$  was considered significant.

*All supplementary materials are available online at [www.molmed.org](http://www.molmed.org).*

## RESULTS

### In Vitro Characterization of Human SkmSCs

We characterized five human SkmSC lines to verify their proliferative and differentiative potential (7). Under serum-free culture conditions, we were able to isolate a homogeneous SkmSC population with human MSC-like morphology that grew as adherent cultures. As SkmSCs gradually continued to grow and reached confluency, they were constantly collected to count the cell number with Trypan Blue Assay. As a result, we ob-

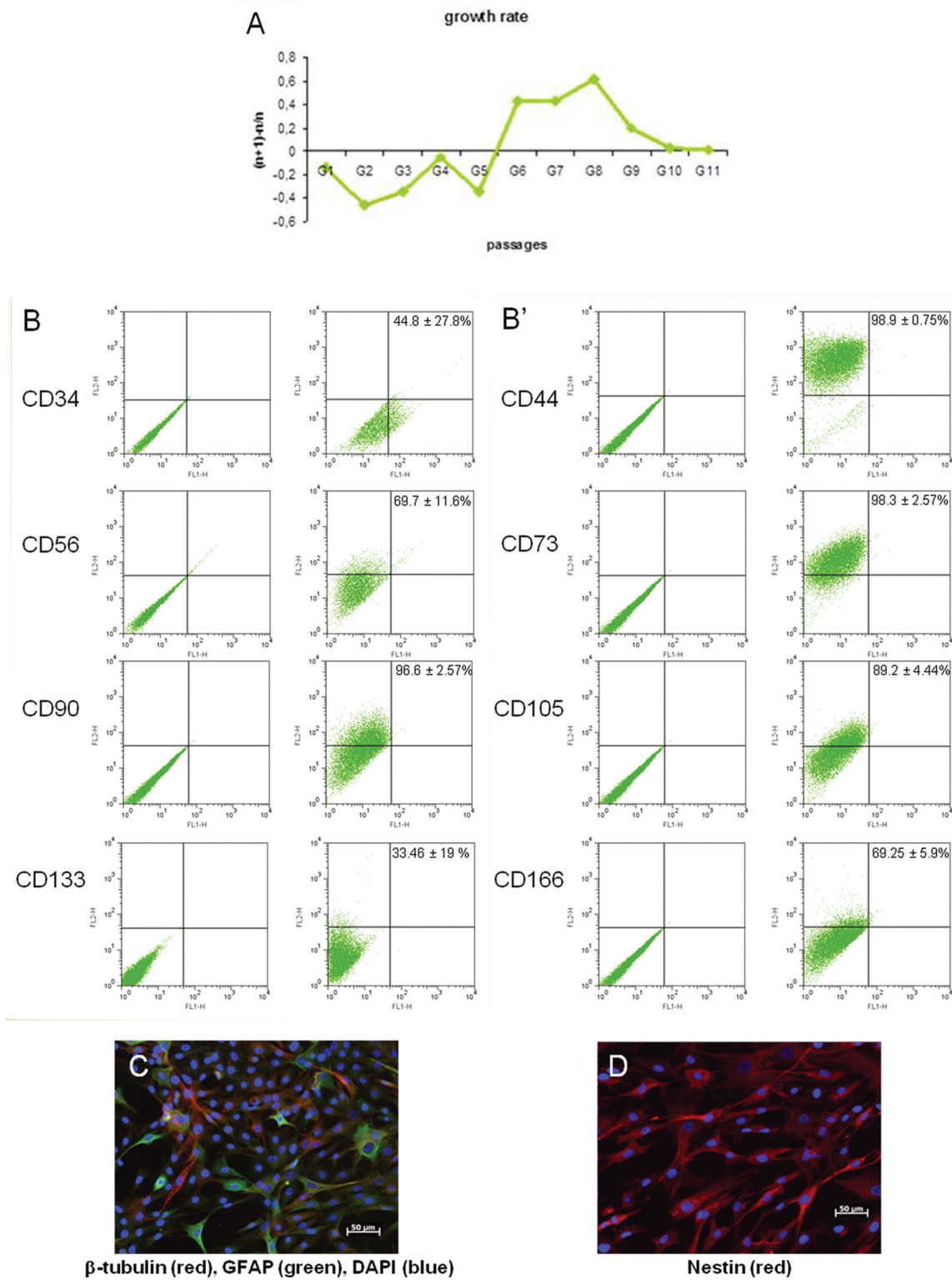


**Figure 1.** *In vitro* characterization of SkmSCs. (A) Growth rate of SkmSCs: growth rate =  $(n + 1) - n/n$  values;  $n$  = number of passage. (B and B') FACS analysis of SkmSCs. (C) Differentiated SkmSCs stained positively for  $\beta$ -tubulin-III (red) and GFAP (green). (D) Immunostaining for Nestin (red). DIV, days *in vitro*. All nuclei were counterstained with 4'-6-diamidino-2-phenylindole (DAPI) (blue). Results are representative of five different SkmSC lines. Results are displayed as means  $\pm$  SD. (C, D) Scale = 50  $\mu$ m.



served that SkmSCs kept in culture for several weeks (up to 20 passages *in vitro* [P20]) maintain a stem cell-like proliferation profile (Figure 1A). The immunophenotypic analysis by FACS of this cell population showed that a high percentage of the SkmSCs (P8–10) expressed characteristic cluster of differentiation (CD) markers of MSCs, for example, CD105 ( $89.18 \pm 4.44\%$ ), CD73 ( $98.27 \pm 2.57\%$ ), CD90 ( $96.59 \pm 2.57\%$ ), CD44 ( $98.9 \pm 0.75\%$ ), CD166 ( $69.25 \pm 5.95\%$ ) and CD56 ( $69.7 \pm 11.6\%$ ) (Figures 1B, B') (24).

However, hematopoietic stem cell CD markers seemed to be present in a lower fraction in human SkmSCs (P8–10), for example, CD34 ( $44.8 \pm 27.8$ ) and CD133 ( $33.5 \pm 19.1$ ) (see Figures 1B, B'). This result suggested a common precursor between the hematopoietic and mesenchymal lineages (25).

Human SkmSCs, when induced with neural differentiation media for 7 d, started showing morphological changes suggestive of cells of astrocytic/neuronal lineages by d 4 and appear highly positive for the neural stem cell marker Nestin, for example ( $99.34 \pm 0.2\%$ ) (Figure 1D). At 7 d after neural differentiation conditions, the distribution of immunoreactivity against GFAP and  $\beta$ -tubulin-III was both high and intense, confirming the neurogenic potential of the human SkmSCs.

A small number of human SkmSC  $\beta$ -tubulin-III-positive cells also appeared to be positively immunoreactive with GFAP, for example,  $\beta$ -tubulin-III ( $44.62 \pm 7.4\%$ ) and GFAP ( $87.97 \pm 9.5\%$ ) (Figure 1C). At this time, a subset of cells coexpressed neuronal ( $\beta$ -tubulin-III) and glial marker GFAP, indicating that these human SkmSC samples might be in the progenitor stage (or glioblast) of neurogenic differentiation ( $\beta$ -tubulin-III/GFAP  $39.9 \pm 6.8\%$ ) (see Figure 1C) (26).

#### ***In Vitro* Labeling of SkmSCs with SPIO and Poly-L-Lysine Transfect Agent**

We observed that SPIO labeling of SkmSCs was feasible and did not impair cell viability or biological characteristics *in vitro* (Figures 2A, A').

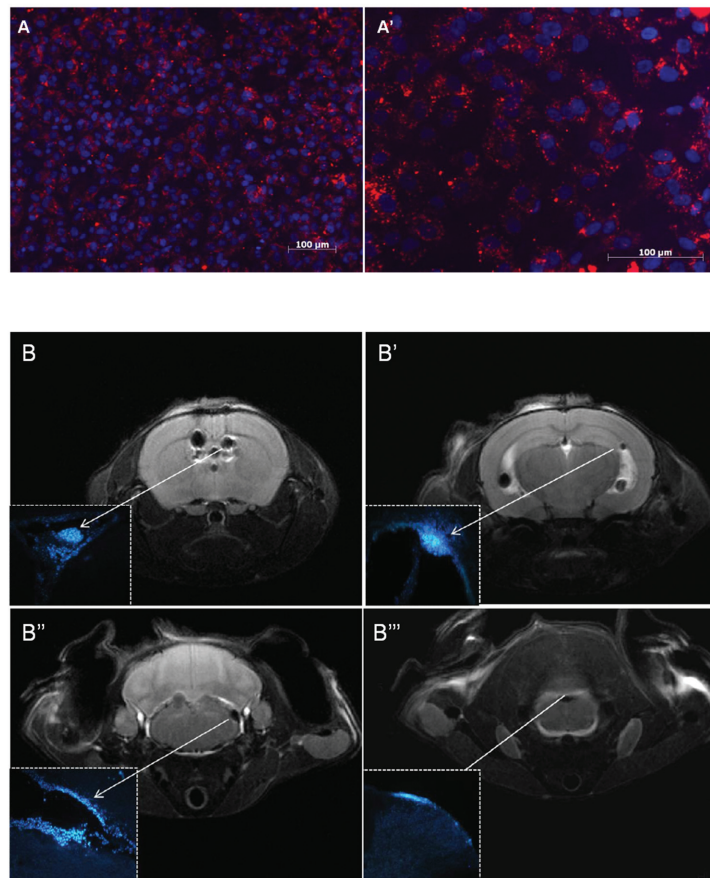


**Figure 2.** SkmSC SPIO internalization and *in vivo* MRI tracing. (A, A') SPIO-labeled SkmSCs stained with an anti-dextran antibody (red) and counterstained with a viable cells dye Hoechst 33258 (blue) for quantitative and qualitative analysis of SPIO labeling efficiency; scale = 100  $\mu$ m. (B–B''') *In vivo* MRI of Wr mice brain postgrafted with Hoechst/SPIO-double labeled SkmSCs 1 wk after injection.

#### ***In Vivo–Ex Vivo* Correlation of SkmSCs Tracking Hoechst/SPIO Double Labeling**

The double labeling of SkmSCs with fluorescent (Hoechst 33258) and SPIO tracers allowed us to evaluate the possible anatomical correspondence between the hypointense signal associated with the presence of iron oxide and the fluorescence related to the living nuclear dye. MRI analyses, performed 1 d after cell transplantation, showed hypointense areas corresponding to the ventricular system. These results were similar to result observed in animals only receiving the SPIO-labeled human SkmSCs (Figures 3A, B) and were observed for all transplanted Wr mice.

Figures 2B and B''' show four different representative images of axial MRI slices, 1 wk after cell transplantation, corresponding to the anterior body of lateral ventricles (see Figure 2B), the body of lateral ventricles close to the hippocampus (see Figure 2B') and the periaqueductal gray and cistern magna in the cerebellum and brainstem (see Figure 2B''). Interestingly, the observation of spinal cord slices revealed that a relevant amount of Hoechst-positive nuclei was localized in the external surface. This result could likely be associated with meningeal layers (see Figure 2B'''). The MRI analysis confirmed the pattern of SPIO distribution observed 1 d after cell transplantation. In addition, highly magnified

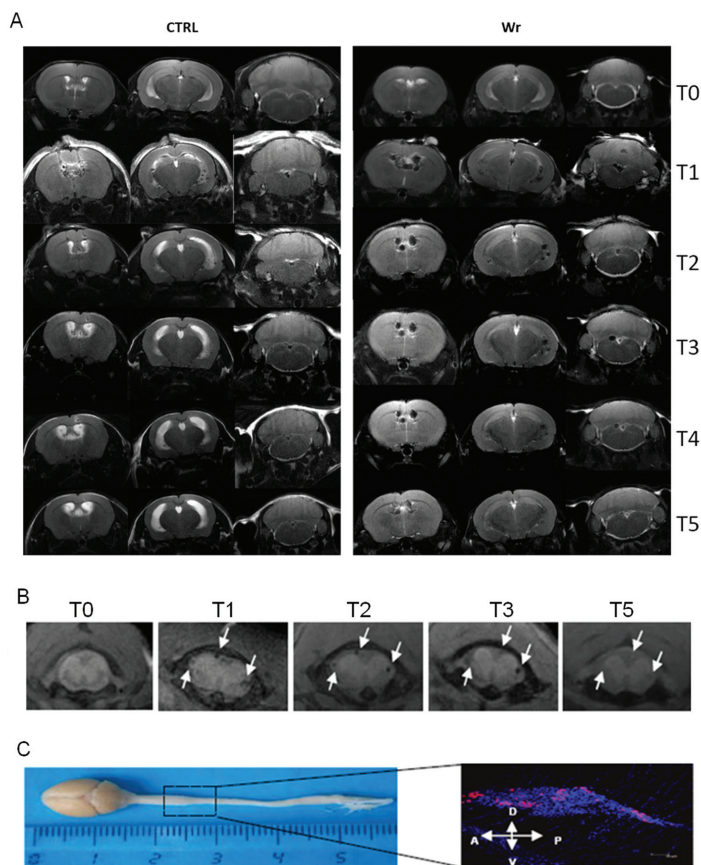


**Figure 3.** Long-term monitoring of SPIO-labeled SkmSCs. (A, B) Representative MRI axial sections of T2-weighted images mouse brains (A) and T1-weighted images cervical spinal cord (B). (C) Photograph of Wr CNS. The immunostaining of Wr whole-mount spinal cord cervical region with anti-human nuclei (AHN) staining (mouse monoclonal antibody (mAb) anti-human nuclei; Chemicon, Temecula, CA, USA; 1:250) (red) 18 wks after transplant. All nuclei were counterstained with DAPI. T0 = MRI acquisition of pretransplanted mouse brain (4 wks of age); T1 = 0 h posttransplant (4 wks of age); T2 = 2 wks posttransplant (6 wks of age); T3 = 4 wks posttransplant (8 wks of age); T4 = 8 wks posttransplant (12 wks of age); T5 = 14 wks posttransplant (18 wks of age).

pictures showed the presence of Hoechst 33258–positive nuclei corresponding to ventricular compartments characterized by a strong decay of signal intensity (see Figure 2B, B', lower-left insert). Although several spinal cord sections analyzed from Wr mice 1 and 6 d after transplantation displayed a relevant number of Hoechst 33258–positive nuclei, we did not find a migration of fluorescent cells to the gray matter and, in particular, in the ventral horns (data not show).

In spite of a small decay of SPIO-induced hypointense signal detected by MRI, a drastic reduction in both the in-

tensity and the overall number of Hoechst 33258–positive nuclei was observed in the ventricular system of Wr mice 8 wks after human SkmSC transplantation (data not show). This apparent dichotomy among the two different approaches of cell tracking could likely be due to the bleaching of fluorescent dye or the detachment of bysbenzimidazole molecules from the minor groove of DNA.

The immunostaining results of Wr brains 18 wks after human SkmSC transplantation showed only a modest human SkmSC integration in the brain parenchyma, as confirmed by the pres-

ence of cells immunoreactive for the human-nuclei and carboxy-dextran (data not show).

### Clinical Outcome

From the fourth to the eighth week of life, the body weight increase was similar between the Wr mice transplanted with human SkmSCs and the group receiving PBS alone. In the last week of clinical observation, the group of treated mice showed a higher trend than that of vehicle-treated mice, but this difference did not statistically differ among the two groups (Figure 4A). The rapid and progressive alteration of forepaw adduction observed in Wr mice receiving PBS intracerebroventricularly was greatly attenuated by human SkmSC transplantation (Figure 4B). The beneficial effect was already found at the first week after transplantation and was maintained for the whole duration of clinical observation. The attenuation of the degree of forelimb muscle atrophy was accompanied by a significant improvement of muscular strength in Wr mice transplanted with human SkmSCs (Figure 4C). The significant difference in terms of muscular strength between the two experimental groups occurred at the sixth week of life and was protracted until the end of the study.

### Histopathology of Human SkmSCs Transplanted Wr Mice

Representative images of ChAT-positive motor neurons in the cervical spinal cord from 9-wk-old healthy mice (Figure 4D) and from age-matched Wr mice (Figure 4E) clearly show the marked process of degeneration occurring in affected mice. A reduction of ~60% of ChAT-positive neurons was found in the cervical spinal cord Wr mice receiving PBS alone ( $12.6 \pm 1.32$  mean motor neurons (MNs)  $\pm$  standard error of the mean [SE] for each section) compared with age-matched healthy mice ( $32.6 \pm 2.7$ ). The transplantation with SkmSCs did not lead to a reduction in the rate of motor neuron death at the cervical spinal cord level of 9-wk-old Wr mice ( $12.4 \pm$

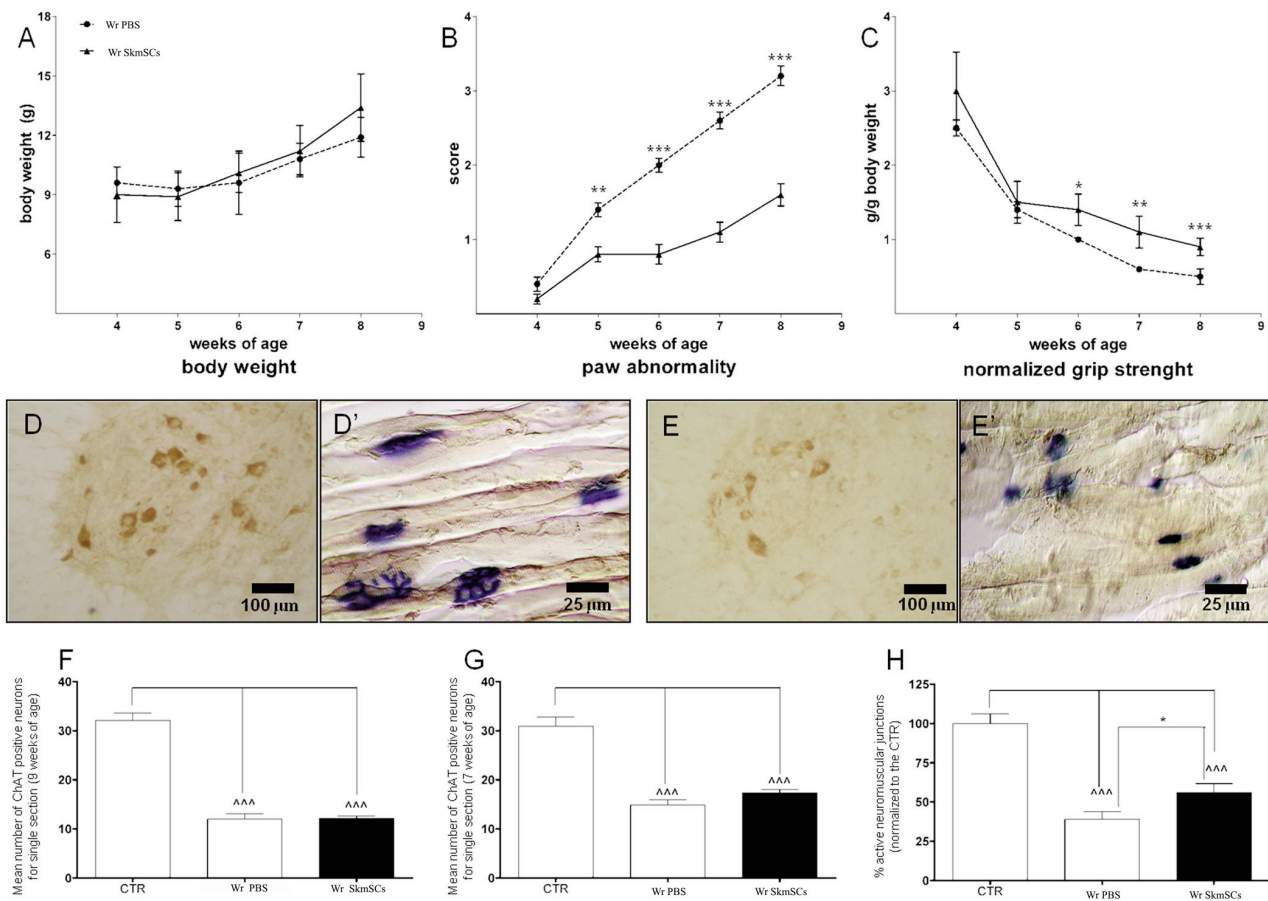


**Figure 4.** Clinical outcome and histopathology of human SkmSC-transplanted Wr mice. (A–C) Behavioral scores of Wr mice that received human SkmSCs or vehicle. Each point represents the mean  $\pm$  SD of 15 animals per group. —●—, Wobbler PBS; —▲—, Wobbler SkmSCs. (D, E) Representative immunohistochemistry of ChAT-positive motor neurons in cervical spinal cord from 9-wk-old healthy mice (D) and from age-matched Wr mice (E); scale = 100  $\mu$ m. (D' and E') Representative view of biceps muscle fibers in both healthy (D') and Wr mice (E'); scale = 25  $\mu$ m. Bromo indoxyl acetate (blue). (F–H) Histograms showing the values of ChAT-positive motor neurons and active neuromuscular junctions. Data represent mean  $\pm$  SD of 14 replications. \* $P$  < 0.05; \*\* $P$  < 0.01; \*\*\* $P$  < 0.0001; ^^^ $P$  < 0.0001. Q36. CTR, Control healthy mice.

0.4). The counting of ChAT-positive motor neurons, performed at an earlier stage of symptom progression (at the seventh week of age), did not show a significant difference between Wr mice transplanted with SkmSCs ( $14.9 \pm 1.3$ ) and PBS-treated Wr ( $17.4 \pm 1.9$ ) and also revealed a trend of protection in mice receiving cells ( $P = 0.0715$ ).

Figures 4D' and E' show a representative view of biceps muscle fibers in both healthy (see Figure 4D') and symptomatic Wr mice (see Figure 4E'). The comparison between the two images reveals a marked alteration in the integrity of muscle fibers and a hypotrophy of neuromuscular junctions. In

accordance with this observational result, we found a drastic reduction on the percentage of active neuromuscular junctions in 7-wk-old Wr mice compared with their age-matched controls (the percentage of healthy mice was normalized and expressed as 100). However, a little but significant preservation was found in mice treated with SkmSCs ( $56.3 \pm 1.9$ ) compared with PBS-treated age-matched Wr mice ( $39.9 \pm 6.0$ ) (\* $P = 0.221$ ). We also examined the migration of transplanted SkmSCs. Histograms showing the values of ChAT-positive motor neurons and active neuromuscular junctions are shown in Figures 4F–H.

### Molecular Characterization of SkmSC Regenerative Proprieties

To characterize the molecular factors involved in therapeutic proprieties of human SkmSCs in the Wr mice, we performed a human gene expression profile of the regulation of key genes involved in the neurogenesis processes and in the inflammatory response in total brains and spinal cords of 6-wk-old Wr mice (2 wks after human SkmSC transplant). We focused our analysis on changes in gene expression higher than fourfold (Table 1). We also performed a human protein expression analysis to confirm the production of human interleukin (IL)-10 and IL-13 proteins in



**Table 1.** Gene and protein expression profile of human Skmsc-transplanted Wr CNS.

Human antiinflammatory cytokines and receptors			
Gene	Fold difference	P	
Decreased gene expression			
<i>CCL2</i>	-5.5996	0.000189	
<i>CXCL2</i>	-255.7635	0.004607	
<i>CXCL6</i>	-447.3727	0.003429	
<i>IL-1R1</i>	-563.6543	0.00016	
Increased gene expression			
<i>IL-10</i>	4812.82	0.000001	
<i>IL-10RA</i>	950.582	0.015	
<i>IL-13</i>	21658.8	0.015	
Bio-Plex cytokine assay			
Protein	Average fluorescence intensity	SD	P
IL-13	9.82	0.606	0.038611
IL-10	0.56	0.737	0.18

Gene expression profile: Results are expressed in fold change signal between *in vitro* Skmscs, vehicle-treated Wr CNS and Skmsc-transplanted Wr CNS. Values are expressed as mean ± SD. *P* < 0.05 for human Skmsc-transplanted Wr CNS versus human Skmscs cultured *in vitro*. Protein expression profile: Results are expressed in average fluorescence intensity signal between Skmsc-transplanted Wr CNS and vehicle-treated Wr CNS. Values are expressed as mean ± SD. *P* < 0.05 for human Skmsc-transplanted Wr CNS versus vehicle-treated Wr CNS.

human Skmsc transplant Wr mice (Table 1).

Immunofluorescent experiments at the cervical spinal cord level of both 7-wk-old Wr mice treated with Skmscs (Figures 5B, B'') and age-matched PBS-treated Wr mice (Figures 5A, A'') confirmed the relevant process of as-

trogliosis occurring during disease progression. However, although Skmscs did not arrest the process of hypertrophy of astrocytes (Figures 5B', C'), a mild attenuation of microglia activation (monitored by the expression of CD11b) seems to be produced by cell transplantation (Figures 5C, C').

**DISCUSSION**

In this study, a total of 500,000 human Skmscs were injected into the intracerebroventricular space of 4-wk-old Wr mice to assess their therapeutic value in reducing the pathology in the Wr mouse model of ALS. Treated Wr mice did exhibit significant improvements in motor function, although none of these mice approached the functional capabilities of wild-type mice. The choice of Skmscs with MSC distinctiveness as a possible cell therapy in motor neuron disorders is closely related to previous experimental evidence on MSC treatments for central nervous system (CNS) diseases (27).

Recent studies have revealed that the hypothesized mechanism of MSC action seems to be related to the release of protective factors, even far from the injured site, rather than the actual replacement of degenerating neurons. Such a therapeutic effect may be provided by different classes of molecules, including trophic factors, antiinflammatory cytokines and immunomodulatory chemokines released from transplanted cells (28).

Four main results emerged from the present study: (a) Skmscs spread in the whole ventricular system and survive inside the ventricles for a long time, and this survival is more prolonged in Wr mice than in controls; (b) in both Wr and healthy mice, transplanted Skmscs do not significantly integrate in the brain parenchyma; (c) despite the lack of evidence of Skmsc migration to the affected Wr cervical spinal cord parenchyma, cell transplantation significantly improved motor activity; (d) the therapeutic effects of Skmscs, which persisted until the end of the behavioral observation, are not related to a marked motor neuroprotection but are likely associated with an immunomodulatory effect.

The efficacy of the intracerebroventricular administration of stem cells in the murine models of neurodegenerative disease has been documented (29). The flux of cerebrospinal fluid in the different districts of the CNS represents one of the main advantages of intracerebroventricu-

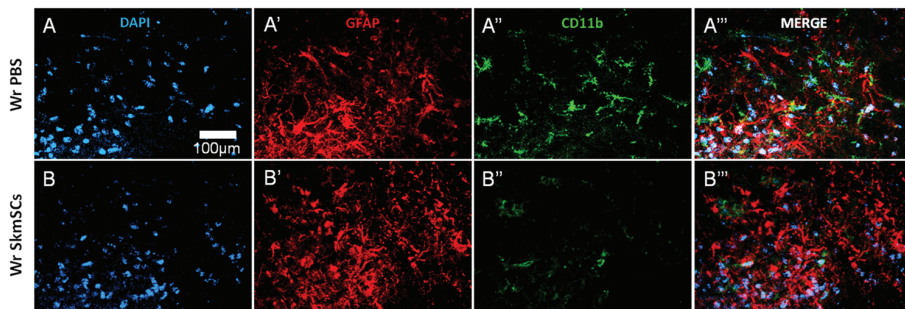


**Figure 5.** Neuropathology of human Skmsc-transplanted Wr mice: astrogliosis and microglial activation. Immunostaining for GFAP (red) and CD11b (green) at the cervical spinal cord level of both 7-wk-old Wr mice treated with Skmscs (B-B'') and age-matched PBS-treated Wr (A-A'') are shown. All nuclei were counterstained with DAPI (blue). Scale = 100 µm.



lar transplantation. On the other hand, this approach requires a detailed investigation on the interaction between transplanted cells and host tissue. The internalization of SPIO has already been demonstrated to be an efficient, reliable, safe and long-lasting procedure to visualize stem cells at different times after transplantation in the CNS of rodents and to follow their migration or disappearance. In the present study, MRI analysis, weekly performed in both Wr and healthy littermates after transplantation, showed that human SkmSCs rapidly spread along the ventricular system (third ventricle, body and posterior horns of lateral ventricles, cisterna magna, fourth ventricle, meningeal layers) in both groups (see Figure 3A). The longitudinal observation revealed an overall decrease of the signal for both groups (see Figure 3A). However, in the brain of Wr mice, the decay was delayed and lower compared with healthy mice (see Figure 3A). The reason why transplanted SPIO-labeled SkmSCs remain in diseased mice for a longer time is far from clear. The hypothesis is that chemoattractant factors, released from injured neurons or activated glial cells, may somehow favor the permanence of transplanted cells. However, this intriguing hypothesis seems to be in part mitigated by the evidence of the almost complete lack of a selective migration of SkmSCs in the affected ventral horns of cervical spinal cord in Wr mice. To localize the engrafted human SkmSCs with a higher level of resolution, the vital nuclear intercalant (Hoechst 33258) was used to label the cells before the transplantation in the Wr brain ventricles. In both Wr and healthy littermates, a relevant amount of Hoechst 33258-positive cells were found to be confined to the ventricular system. A large number of Hoechst 33258 fluorescent nuclei was found at the cervical region 1 wk after SkmSC transplantation. The nuclei were mainly localized close to the dorsal white matter or attached to the meningeal layer. Their presence in cervical spinal cord sections of Wr mice until the sixth

week after transplantation may favor a possible cross-talk between SkmSCs and affected Wr regions. The overlapping between the SPIO-related signal, MRI slices, the presence of Hoechst 33258 nuclei and histology confirmed the almost exclusive localization of SkmSCs inside the ventricle layers.

Our *in vitro* studies have shown that SkmSCs express some important markers of neural lineage (see Figures 1C, D). However, the lack of apparent cell migration to the side of injury (ventral horn of the Wr cervical spinal cord) and the absence of their differentiation toward motor neurons did not allow us to speculate that there is a cell replacement by SkmSCs. Whereas other MSC transplantation studies in ALS animal models demonstrate a motor efficacy improvement without grafts replacement, we have chosen to focus our investigation on the evaluation of the SkmSC pharmacological effects (9).

Here we first report the reliability of this dual modality of fluo-paramagnetic labeling of stem cells for *in vivo* and *ex vivo* tracking. Although the loading of SPIO and Hoechst 33258 is not reported to be associated with mechanisms of cytotoxicity, the transplantation of SkmSCs in Wr mice for clinical estimation was performed by avoiding their prelabeling with exogenous tracers. We opted for this approach for two main reasons: a practical reason (we suppose that the possible future application of cell therapy in humans will not consider labeled cells) and an experimental reason (we previously demonstrated the reliability of *ex vivo* tracking with antibodies directed against endogenous markers). It was recently reported that the recruitment of a relatively low number of animals is considered one of the main factors responsible for the “lost in translation” between the results obtained from trials in the SOD1 mouse and in human ALS (30). Generally, to avoid the rejection of human cells, cyclosporine is given from the day of transplantation to the end of symptoms. However, the inhibition of immune response by cy-

closporine A may play a therapeutic role by acting as an antiinflammatory agent or by reducing mitochondrial impairment and cell death in neurons (31). Because of the low immunogenicity of the fetal SkmSCs, the present study was carried out in the absence of immunomodulant agents so we could avoid any possible bias due to interaction between cyclosporine A and SkmSC transplant effects.

In our study of SkmSC tracking, which lasted for over 3 months, after cell transplantation for both Wr mice and healthy controls, the lack of cyclosporine A did not lead to acute toxicity and/or higher mortality compared with untreated littermates.

In our study, Wr mice receiving SkmSCs rapidly and significantly showed reduced progression of foreleg atrophy and, therefore, as a consequence, suffered less loss of forelimb muscular strength. The transplantation of SkmSCs seemed to produce a faster and stronger outcome in comparison with our previous results obtained by intraperitoneally injecting Riluzole in Wr mice (32).

On the other hand, in contrast to the results obtained by Riluzole treatment, SkmSC transplantation did not significantly preserve the rate of motor neuron loss at the end stage of our study (see Figures 4F, H).

## CONCLUSION

The beneficial effect emerging from this study, therefore, may be explained by the production and secretion of a variety of growth factors, cytokines and chemokines that could play a beneficial role in maintaining a functionality in the survived motoneurons.

The link between the immunomodulant and therapeutic effects of MSCs on ALS animal models has already been hypothesized (9). In particular, the analysis of the levels of cytokines measured in vehicle-treated ALS mice and in ALS mice receiving cells suggested that transplantation may favor the maintenance of Th-2 innate adaptive immune response by delaying the switch to the Th1-mediated pro-

inflammatory response and therefore attenuating the clinical progression (9).

The role of proinflammatory cytokines in exacerbating pathological and clinical features of ALS has already been described in patients, animals and neuronal cultures (32). Here, we first report the expression levels of a panel of human specific anti-cytokines-chemokines, expressed by SkmSCs 2 wks after intracerebroventricular transplantation in lateral ventricles of Wr mice.

The RT and protein profiler analysis of human SkmSC-transplanted Wr in brain revealed that several factors involved in the antiinflammatory response, such as human IL-10 and its receptor IL-10RA (IL-10 receptor  $\alpha$ ) (33), are highly expressed (Table 1) and that their expression is increased *in vivo* compared with *in vitro*. The IL-10 gene encodes for the antiinflammatory cytokine of type 2 helper T cells (34). IL-10 is a potent inhibitor of inflammation because of its ability to reduce T-cell activity and subsequent inflammatory cytokine production. In the past 10 years, the beneficial effects of IL-10 was observed in several neuroinflammatory disease models (35). Interestingly, an increase of IL-10 and a shift from Th1 to Th2 response has been similarly described in SOD1G93A mice receiving human umbilical cord blood (hUCB) cells and showing a therapeutic benefit. IL-13 is also involved in the antiinflammatory process by means of similar mechanisms described above for IL-10 (33).

In the brainstem and spinal cord of both patients with ALS and Wr mouse models, increasingly, many activated microglia and astrocytes, IgG and T lymphocytes may be capable of secreting the numerous cytokines that play key roles in the inflammatory reaction (32). The increase of macrophage-cytokines such as IL-1 $\alpha$ , IL-1 $\beta$  and IL-1RA and the up-regulation of the tumor necrosis factor (TNF) gene make them likely candidates for inflammatory effectors (32). IL-10 and IL-13 inhibit the production of several proinflammatory cytokines including TNF and IL-1 $\beta$  in monocytes and macrophages (33). It is therefore impor-

tant to underline that, in Wr mice, the levels of TNF- $\alpha$  at the cervical spinal cord region rapidly increase at the early symptomatic phase and are accompanied by a parallel increase of two important downstream stress kinases (p-JNK and p-P38) having potential neurotoxicity (36). It has also been reported that the chronic treatment with a soluble receptor for the tumor necrosis factor receptor 1 (TNFR1) (Onercept), which had already shown antiinflammatory activity in peripheral districts, drastically reduced the symptom progression in Wr mice (36).

The main indication emerging from our study is that SkmSCs have a bystander effect by releasing some important antiinflammatory cytokines far from the pathological areas. Thus, we hypothesize that a deeper comprehension of the mechanisms involved in the beneficial effects observed after human SkmSC treatment could open a new prospective on the formulation of a practical, safe and potential therapeutic strategy for patients with ALS.

#### ACKNOWLEDGMENTS

We are grateful to Andrea Smith for the helpful review of the English in the manuscript. We also thank Giulio Alessandri and Giorgio Battaglia for critically reading this scientific article. This work was supported by IRCCS Foundation Neurological Institute "C. Besta" (LR8) and by the Italian Ministry of Health (RF-INN-2007-644440).

#### DISCLOSURE

The authors declare that they have no competing interests as defined by *Molecular Medicine*, or other interests that might be perceived to influence the results and discussion reported in this paper.

#### REFERENCES

- Boillee S, Cleveland DW. (2008) Revisiting oxidative damage in ALS: microglia, Nox, and mutant SOD1. *J. Clin. Invest.* 118:474–8.
- Wokke J. (1996) Riluzole. *Lancet.* 348:795–9.
- Lodi D, Iannitti T, Palmieri B. Stem cells in clinical practice: applications and warnings. *J. Exp. Clin. Cancer Res.* 30:9.

- Justesen J, Stenderup K, Eriksen EF, Kassem M. (2002) Maintenance of osteoblastic and adipocytic differentiation potential with age and osteoporosis in human marrow stromal cell cultures. *Calcif. Tissue Int.* 71:36–44.
- Jiang Y, et al. (2002) Pluripotency of mesenchymal stem cells derived from adult marrow. *Nature.* 418:41–9.
- Sanchez-Ramos J, et al. (2000) Adult bone marrow stromal cells differentiate into neural cells in vitro. *Exp. Neurol.* 164:247–56.
- Alessandri G, et al. (2004) Isolation and culture of human muscle-derived stem cells able to differentiate into myogenic and neurogenic cell lineages. *Lancet.* 364:1872–83.
- Gotherstrom C, et al. (2004) Immunologic properties of human fetal mesenchymal stem cells. *Am. J. Obstet. Gynecol.* 190:239–45.
- Garbuzova-Davis S, et al. (2008) Human umbilical cord blood treatment in a mouse model of ALS: optimization of cell dose. *PLoS One.* 3:e2494.
- Falconer DS. (1956). *Mouse News Letter.* 15:23.
- Schmitt-John T, et al. (2005) Mutation of Vps54 causes motor neuron disease and defective spermiogenesis in the wobbler mouse. *Nat. Genet.* 37:1213–5.
- Fumagalli E, Bigini P, Barbera S, De Paola M, Mennini T. (2006) Riluzole, unlike the AMPA antagonist RPR119990, reduces motor impairment and partially prevents motoneuron death in the wobbler mouse, a model of neurodegenerative disease. *Exp. Neurol.* 198:114–28.
- Palmisano R, et al. (2011) Endosomal accumulation of APP in wobbler motor neurons reflects impaired vesicle trafficking: implications for human motor neuron disease. *BMC Neurosci.* 12:24.
- Wada MR, Inagawa-Ogashiwa M, Shimizu S, Yasumoto S, Hashimoto N. (2002) Generation of different fates from multipotent muscle stem cells. *Development.* 129:2987–95.
- Neri M, et al. (2008) Efficient in vitro labeling of human neural precursor cells with superparamagnetic iron oxide particles: relevance for in vivo cell tracking. *Stem Cells.* 26:505–16.
- D.L. no. 116, G.U. suppl. 40, 18 February 1992.
- Circolare no. 8, G.U., 14 Luglio 1994.
- EEC Council Directive 86/609, OJ L 358, 1, Dec. 12, 1987.
- Institute of Laboratory Animal Resources; Commission on Life Sciences; National Research Council. (1996) *Guide for the Care and Use of Laboratory Animals*. Washington (DC): National Academy Press. Available from: [http://www.nap.edu/openbook.php?record\\_id=5140](http://www.nap.edu/openbook.php?record_id=5140)
- Rathke-Hartlieb S, Schmidt VC, Jockusch H, Schmitt-John T, Bartsch JW. (1999) Spatiotemporal progression of neurodegeneration and glia activation in the wobbler neuropathy of the mouse. *Neuroreport.* 10:3411–6.
- Mennini T, et al. (2006) Nonhematopoietic erythropoietin derivatives prevent motoneuron degeneration in vitro and in vivo. *Mol. Med.* 12:153–60.

22. Bigini P, Mennini T. (2004) Immunohistochemical localization of TNF $\alpha$  and its receptors in the rodent central nervous system. *Methods Mol. Med.* 98:73–80.
23. Bigini P, et al. (2010) Neuropathologic and biochemical changes during disease progression in liver X receptor beta $^{-/-}$  mice, a model of adult neuron disease. *J. Neuropathol. Exp. Neurol.* 69:593–605.
24. Dominici M, et al. (2006) Minimal criteria for defining multipotent mesenchymal stromal cells. The International Society for Cellular Therapy position statement. *Cytotherapy.* 8:315–7.
25. Yin AH, et al. (1997) AC133, a novel marker for human hematopoietic stem and progenitor cells. *Blood.* 90:5002–12.
26. Ogawa Y, et al. (2002) Transplantation of in vitro-expanded fetal neural progenitor cells results in neurogenesis and functional recovery after spinal cord contusion injury in adult rats. *J. Neurosci. Res.* 69:925–33.
27. Cristofanilli M, Harris VK, Zigelbaum A, et al. (2011) Mesenchymal stem cells enhance the engraftment and myelinating ability of allogeneic oligodendrocyte progenitors in dysmyelinated mice. *Stem Cells Dev.* 20:2065–76.
28. Mazzini L, et al. (2010) Mesenchymal stem cell transplantation in amyotrophic lateral sclerosis: a phase I clinical trial. *Exp. Neurol.* 223:229–37.
29. Rehni AK, Singh N, Jaggi AS, Singh M. (2007) Amniotic fluid derived stem cells ameliorate focal cerebral ischaemia-reperfusion injury induced behavioural deficits in mice. *Behav. Brain Res.* 183:95–100.
30. Benatar M. (2007) Lost in translation: treatment trials in the SOD1 mouse and in human ALS. *Neurobiol. Dis.* 26:1–13.
31. Keep M, Elmer E, Fong KS, Csiszar K. (2001) Intrathecal cyclosporin prolongs survival of late-stage ALS mice. *Brain Res.* 894:327–31.
32. Mosley RL, Gendelman HE. Control of neuroinflammation as a therapeutic strategy for amyotrophic lateral sclerosis and other neurodegenerative disorders. *Exp. Neurol.* 222:1–5.
33. Opal SM, Keith JC, Palardy JE, Parejo N. (2000) Recombinant human interleukin-11 has anti-inflammatory actions yet does not exacerbate systemic Listeria infection. *J. Infect. Dis.* 181:754–6.
34. Hoffmann KF, Cheever AW, Wynn TA. (2000) IL-10 and the dangers of immune polarization: excessive type 1 and type 2 cytokine responses induce distinct forms of lethal immunopathology in murine schistosomiasis. *J. Immunol.* 164:6406–16.
35. Qiu F, et al. (2006) [Effect of ligustrazine on cell proliferation in subventricular zone of lateral cerebral ventricle after adult rat suffering from focal cerebral ischemia]. *Sichuan Da Xue Xue Bao Yi Xue Ban* 37:726–9, 780.
36. Bigini P, et al. (2007) Lack of caspase-dependent apoptosis in spinal motor neurons of the wobbler mouse. *Neurosci. Lett.* 426:106–10.